

Electronic Supplementary Information

Sustainable, recyclable and robust elastomers enabled by exchangeable interfacial cross-linking

Min Qiu, Siwu Wu, Shifeng Fang, Zhenghai Tang and Baochun Guo

Content

1. Materials.....	2
2. Diazo-functionalization of CB	2
3. Preparation of CB/ENR composites.....	2
4. Characterizations	3
5. TG curves, FTIR and XPS spectra for CB samples	6
6. Formulations for rubber composites	7
7. Dispersion of CB samples in ethanol	7
8. FTIR spectra of CB- <i>x</i> samples	8
9. Dilatometry and Creep curves for CB- <i>x</i> composites.....	8
10. Strain rate, Young's modulus and relaxation time for CB- <i>x</i> composites.....	9
11. Temperature-dependent relaxation experiment for CB- <i>x</i> composites	10
12. Mechanical properties of CB- <i>x</i> samples and other vitrimer elastomers	11
13. Morphology of CB-20 and CB-40 samples	12
14. Storage modulus and tan δ of CB- <i>x</i> composites	13
15. Vulcanization properties for CB- <i>x</i> composites	14
16. Cross-linking densities of CB- <i>x</i> composites	15
17. Photograph of the original and reprocessed rubber films	15
18. Mechanical properties of original and recycled CB- <i>x</i> composites.....	16
19. FTIR spectra and cross-linking density of original and recycled CB-20.....	17
20. References	18

1. Materials

ENR with an epoxidization degree of 50% (average M_w is 3.59×10^5) was bought from the Agricultural Products Processing Research Institute, Chinese Academy of Tropical Agricultural Science, China. Carbon black (CB, average diameter is 35 nm) were provided by Shanghai Yutong Chemical Technology co. LTD. Zinc acetate ($Zn(Ac)_2$, 98%) and 1, 2-dimethyl-imidazole (DMI, 99%), were purchased from Sigma-Aldrich. Isopentyl nitrite (97%), and 4-aminobenzoic acid (99%) were purchased from Alfa Aesar. N, N'-Dimethyl formamide (DMF) and ethanol were analytically pure and used as received.

2. Diazo-functionalization of CB

Diazo-functionalized CB nanoparticles (g-CB) were synthesized according to the reference with some modification.¹ Briefly, 4 g of CB were dispersed in DMF and sonicated for 30 min. Then, 0.34 mol of 4-aminobenzoic acid was added to the aqueous suspension, and the solution was stirred until complete dissolution of all the reagents. Isopentyl nitrite was dropped to the mixture slowly under stirring for 24 h at 80 °C. Finally, the resultants were thoroughly washed with excess DMF and ethanol to remove unreacted reagents and byproducts, and then dried at 50 °C for 6 h.

3. Preparation of CB/ENR composites

ENR with desired amounts of g-CB, $Zn(Ac)_2$ and DMI were compounded on a two-roll mill (the quantities of $Zn(Ac)_2$ and DMI were 10 mol% and 25 mol% relative to the carboxyl group, respectively). DMI acts as accelerator to promote the cross-linking kinetics,^{2, 3} and $Zn(Ac)_2$ can promote both esterification of epoxy/acids and subsequent transesterification between hydroxyl and ester groups.^{4, 5} The basic formulations are tabulated in Table S1. In the context, sample code of CB- x refers to the sample with x phr (parts per hundred parts of rubber) g-CB. The recycled samples were made by cutting the as-moulded samples into pierces, and then being remolded at 180 °C for certain time determined by the stress relaxation experiment. Specifically, the remolding time for CB-10, CB-15, CB-20, CB-30 and CB-40 samples was 5 min,

10 min, 15 min, 30 min and 90 min, respectively, and the hot pressing pressure is 20 MPa.

For comparison, the biphenyldicarboxylic acid (BDA) cross-linked ENR sample (BDAE, the ratio of oxirane group and carboxyl group is the same as CB-20) was prepared according to the aforementioned protocols.

4. Characterizations

Fourier transform infrared spectroscopy (FTIR) was collected on a Bruker Vertex 70 FTIR spectrometer equipped with a heating cell. Thermal gravimetric analysis (TGA) was performed at a heat rate of 10 °C/min on a TA Q50 machine under nitrogen atmosphere (from 30-700 °C). X-ray photoelectron spectroscopy (XPS) measurements were performed using a Thermo Scientific ESCALAB 250 Multitechnique Surface Analysis equipped with an Al-K α radiation source. Scanning electron microscopy (SEM) images of cryo-fractured surface morphologies were observed with a Hitachi S-4800 FE-SEM microscope. The curing characteristics were determined at 180 °C using a U-CAN UR-2030 vulcameter. Tensile tests were performed on U-CAN UT-2060 (Taiwan) according to ISO standard 37-2005.

The tests including dynamic mechanical analysis (DMA), dilatometry experiments, creep experiments, stress relaxation experiments, and cyclic strain recovery tests were performed with a TA Q800 machine. DMA investigations were performed in a tensile mode at a frequency of 1 Hz and a strain of 0.5%. The test temperature ranged from -40 to 150 °C with a heating rate of 3 °C /min under nitrogen purging. Dilatometry experiments were conducted by measuring the length of sample when it was heated from -50 to 250 °C at 3 °C/min, and a weak stress of 10 kPa was applied to avoid buckling. For creep experiments, a nominal stress of 0.1 MPa was applied on the sample after a 10 min temperature equilibration. Relaxation time τ is calculated from elongational creep experiments (Fig.S4b) according to the following equations: $\eta = \sigma / \dot{\epsilon}$, $\tau = \eta / E$, that is $\tau = \sigma / (\dot{\epsilon} E)$, where η refers to the viscosity (Pa·s), σ presents the stress (Pa), $\dot{\epsilon}$ stands for the strain rate (s⁻¹) and E is the Young's modulus at 180 °C (Pa). The parameters used to calculate the relaxation time were listed in Table S3. σ is

a constant value of 0.1 MPa for all the samples. The strain rate ε' was determined from the slope of the linear fit from creep experiments. E is calculated from the slope of the stress-strain curves (0.5-3% strain) that are measured using DMA Q800 by stretching rectangular samples (10 mm \times 4 mm \times 1 mm) at 180 °C with a load rate of 0.5 N/min. Stress relaxation experiments were also conducted on the DMA machine with 0.3% constant applied, and balanced for half an hour to exclude the influence of thermal expansion. The characteristic relaxation time τ^* was determined as the time required to relax to 37% of the initial relaxation modulus. Characteristic relaxation times τ^* follows an Arrhenius law $\tau(T) = \tau_0 \exp(E_a/RT)$, where τ_0 refers to the characteristic relaxation time at infinite T , E_a represents the activation energy for the transesterification reaction, R is the universal gas constant and T is the temperature of the experiment conducted. For cyclic strain recovery tests, the stress applied on the sample was alternated between 0.1 MPa for 60 min and 0 MPa for 10 min in each cycle.

Crosslinking density was determined by the equilibrium swelling method in toluene and calculated according to the classical Flory-Rehner equation. Briefly, CB samples were swollen in toluene at room temperature for 72 h. Then the solvent was blotted off quickly from the swollen sample surface using filter paper. The samples were immediately weighed and then dried in a vacuum oven at 60 °C until constant weight and then reweighed. The volume (V_r) fraction of ENR in the swollen gel was calculated according to the following equation:⁷

$$V_r = \frac{M_0 \times \varphi \times (1 - \alpha) / \rho_r}{\varphi \times M_0 \times (1 - \alpha) / \rho_r + (M_1 - M_2) / \rho_s}$$

where M_0 is the weight of the sample before swelling; M_1 and M_2 are the sample masses before and after drying, respectively; φ is the weight fraction of the insoluble components; ρ_r and ρ_s are the rubber and solvent densities, respectively.

The elastically active network chain density (V_e), which can be used to represent crosslink density, was calculated by the well-known Flory-Rehner equation:⁸

$$V_e = - \frac{\ln(1 - V_r) + V_r + \chi V_r^2}{V_s (V_r^{1/3} - V_r / 2)}$$

where V_r is the volume fraction of polymer in the swollen sample, V_s is the solvent molar volume (106.5 cm³/mol for toluene), and χ is the Flory-Huggins polymer solvent interaction parameter (0.341 for ENR and toluene),⁹ and V_s is the molar volume of the solvent (106.5 cm³/mol for toluene).

5. TG curves, FTIR and XPS spectra for CB samples

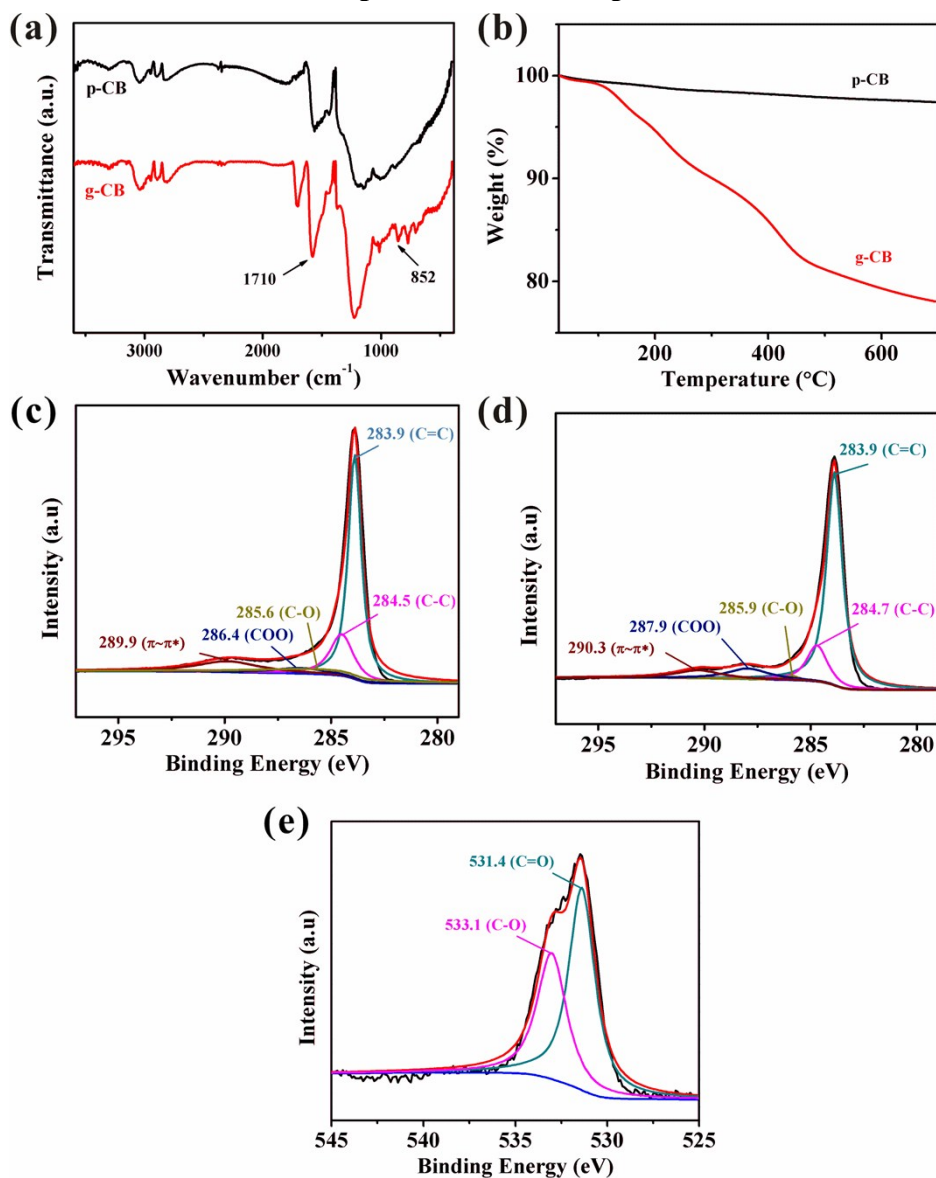


Fig. S1. FTIR spectra a) and TGA curves b) for p-CB and g-CB. High-resolution C 1s XPS spectra of p-CB c) and g-CB d). e) High-resolution O 1s XPS spectra of g-CB.

Table S1. The surface atomic percentages of relevant elements calculated from XPS

high resolution spectra			
	C%	O%	N%
p-CB	98.19	1.81	/
g-CB	87.34	9.09	3.57

6. Formulations for rubber composites

Table S2. Formulations for CB-x samples and BDAE sample

	ENR (phr)	g-CB (phr)	BDA (phr)	Oxirane/carboxyl group mole ratio
CB-10	100	10	/	18
CB-15	100	15	/	12
CB-20	100	20	/	9
CB-30	100	30	/	6
CB-40	100	40	/	4
BDAE	100	/	9	9

7. Dispersion of CB samples in ethanol

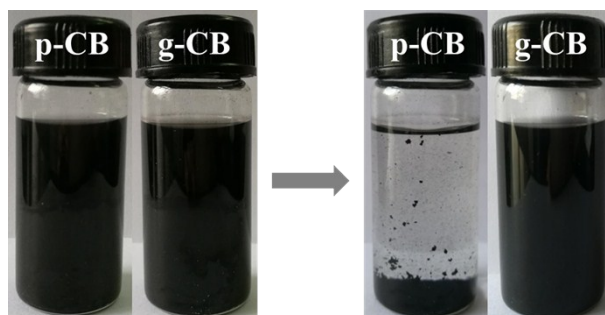


Fig. S2. Dispersion of p-CB and g-CB in ethanol (left: right after sonication, right: after standing for 24 h).

8. FTIR spectra of CB-x samples

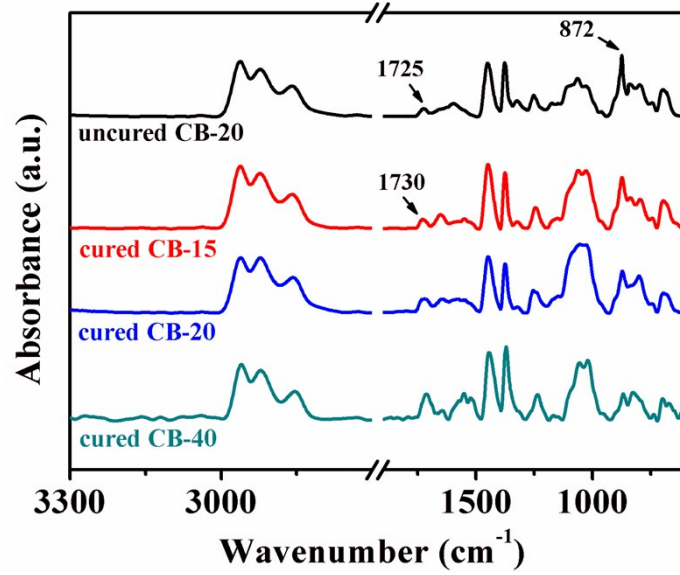


Fig. S3. FTIR spectra of the uncured CB-20, cured CB-15, cured CB-20 and cured CB-40.

9. Dilatometry and Creep curves for CB-x composites

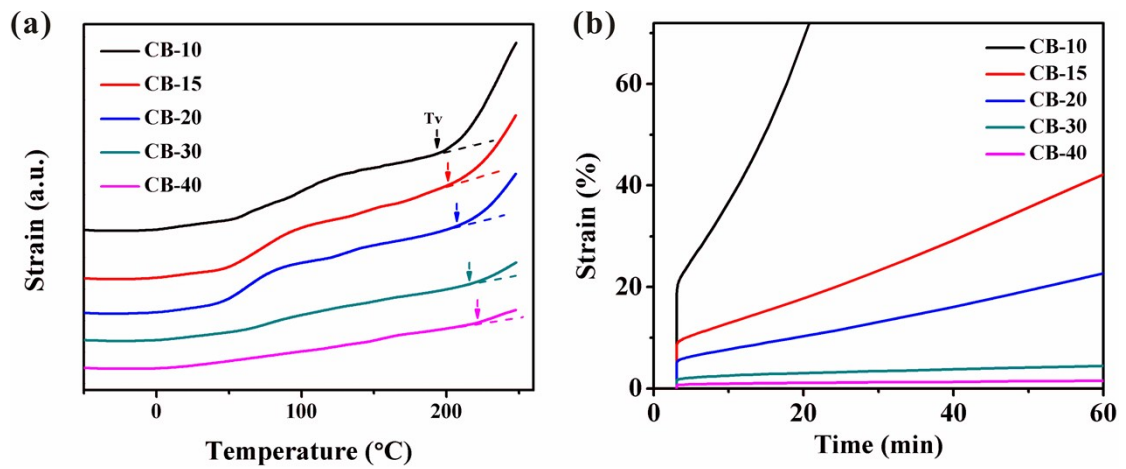


Fig. S4. a) Dilatometry experiments for CB-x samples at a heating rate of 3 °C /min. b) Creep experiments for CB-x samples with a nominal stress of 0.1 MPa at 180 °C.

10. Strain rate, Young's modulus and relaxation time for CB-x composites

Table S3. Strain rate, Young's modulus at 180 °C, and relaxation time for CB-x samples

Samples	$\dot{\varepsilon}$ (10^{-2} min^{-1})	E (Mpa)	τ (min)
CB-10	2.84	0.55	6.5
CB-15	0.58	1.12	15.5
CB-20	0.18	2.05	27.1
CB-30	0.018	4.72	117.8
CB-40	0.004	10.55	237.0

11. Temperature-dependent relaxation experiment for CB-x composites

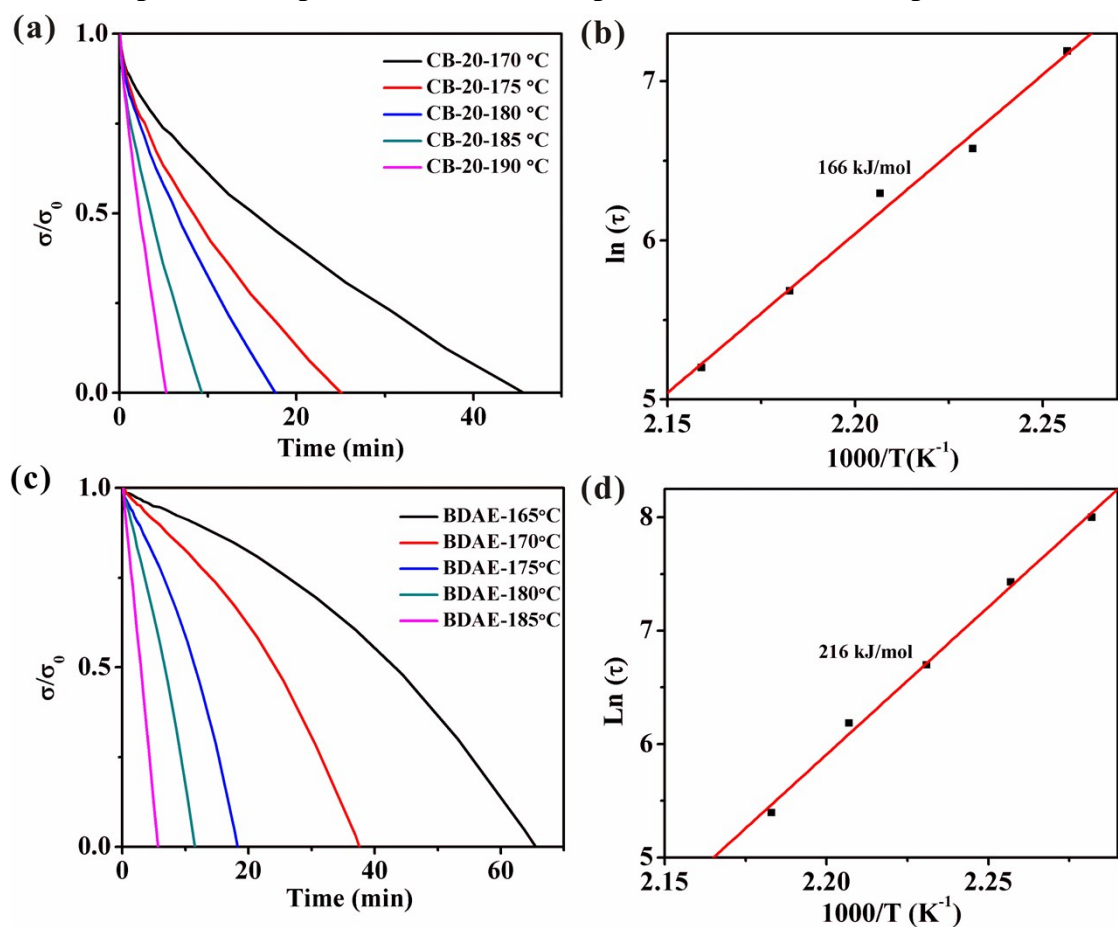


Fig. S5. a) Normalized stress relaxation for CB-20 at various temperatures ranging from 170 to 190 °C with a constant strain of 0.3%. b) Fitting of τ^* to the Arrhenius equation for CB-20. c) Normalized stress relaxation for BDAE sample at various temperatures ranging from 165 to 185 °C with a constant strain of 0.3%. d) Fitting of τ^* to the Arrhenius equation for BDAE sample.

12. Mechanical properties of CB-x samples and other vitrimer elastomers

Table S4. Comparison of mechanical properties between CB-x samples and other vitrimer elastomers

Matrix	Filler	Filler content (phr)	Elongation at break (%)	Tensile strength (MPa)	100% Tensile Modulus (MPa)
ENR	CB	10	517 ± 30	10.3 ± 1.6	1.7 ± 0.1
ENR	CB	15	425 ± 10	13.3 ± 1.3	3.1 ± 0.2
ENR	CB	20	338 ± 13	15.7 ± 1.2	4.8 ± 0.1
ENR	CB	30	184 ± 6	18.1 ± 1.3	11.3 ± 0.3
ENR	CB	40	95 ± 3	22.8 ± 1.9	/
Carboxyl group-grafted butadiene styrene rubber (SBR) ¹⁰	Epoxy group-functionalized silica (SiO ₂)	30	226 ± 16	9.9 ± 0.7	3.29 ± 0.01
Polydimethylsiloxane, cyclohexane dimethanol bisacetoacetate ¹¹	/	/	~ 67	~ 0.072	0.135
Polybutadiene rubber, benzene-1, 3, 5-tricarbaldehyde ¹²	/	/	52 ± 9	0.39 ± 0.02	~ 5.5
Polyurethane, castor oil ¹³	Carbon nanotubes	0.1	~ 340	~ 6.2	/
Polysulfide diglycidyl ether, diethylenetriamine ¹⁴	/	/	~ 105	~ 0.22	~ 0.21
ENR, dithiodibutyric acid ¹⁵	/	/	530	12 ± 2	/
Polybutadiene rubber, sulfur ¹⁶	Si-69 modified SiO ₂	20	~ 380	~ 3.2	~ 1
DGEBA, Pripol 1040 ¹⁷	/	/	~ 170	~ 1.9	~ 1.3

13. Morphology of CB-20 and CB-40 samples

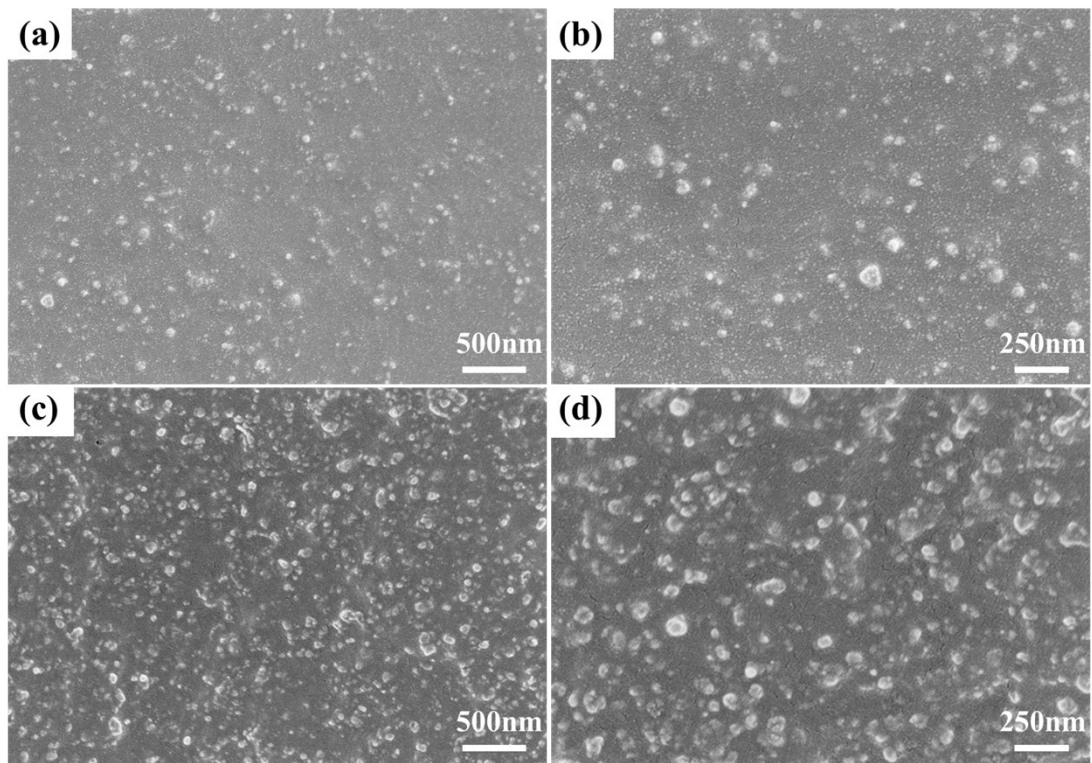


Fig. S6. SEM images of the cryo-fractured surfaces of CB-20 sample (a, b), and CB-40 sample (c, d).

14. Storage modulus and $\tan \delta$ of CB-x composites

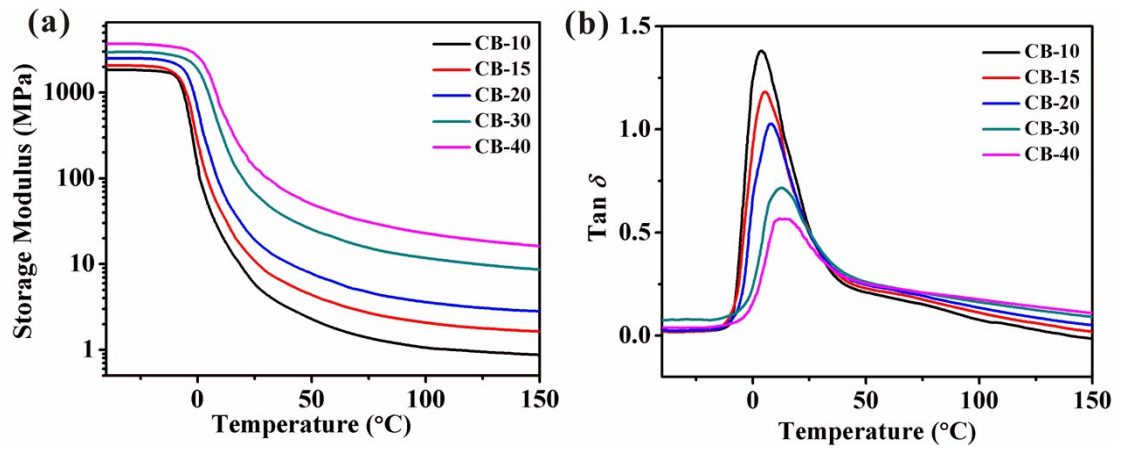


Fig. S7. Storage modulus a), temperature-dependent $\tan \delta$ b) curves of CB-x samples.

15. Vulcanization properties for CB-*x* composites

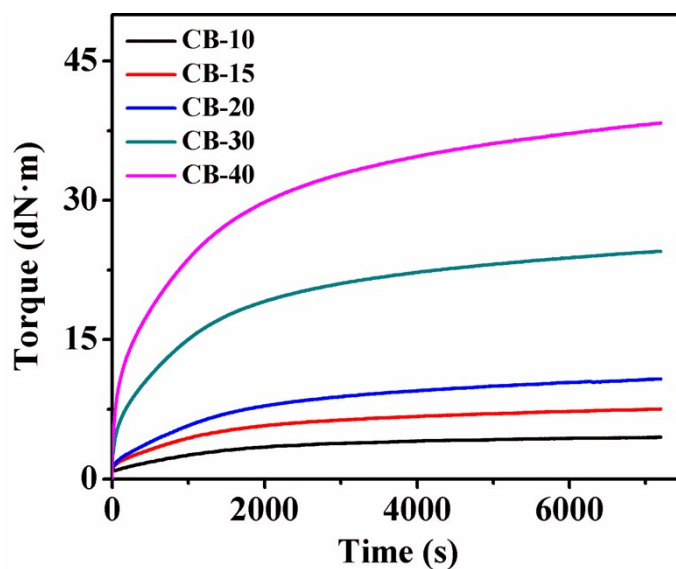


Fig. S8. Vulcanization curves for CB-*x* samples.

Table S5. Experimentally measured values of vulcanization parameters for CB-*x* composites

	TC10 (min)	TC90 (min)	ML (dN·m)	MH (dN·m)	ΔM (dN·m)
CB-10	3:01	72:39	0.87	4.52	3.65
CB-15	2:15	76:52	1.40	7.55	6.15
CB-20	2:08	78:00	1.41	10.78	9.37
CB-30	0:50	67:58	2.66	38.35	35.69
CB-40	0:49	69:08	4.67	59.71	55.04

16. Cross-linking densities of CB-x composites

Table S6. Cross-linking densities of CB-x samples

Samples	Cross-linking density (10^{-5} mol/cm ³)
CB-10	7.3
CB-15	11.6
CB-20	19.4
CB-30	45.3
CB-40	85.7

17. Photograph of the original and reprocessed rubber films

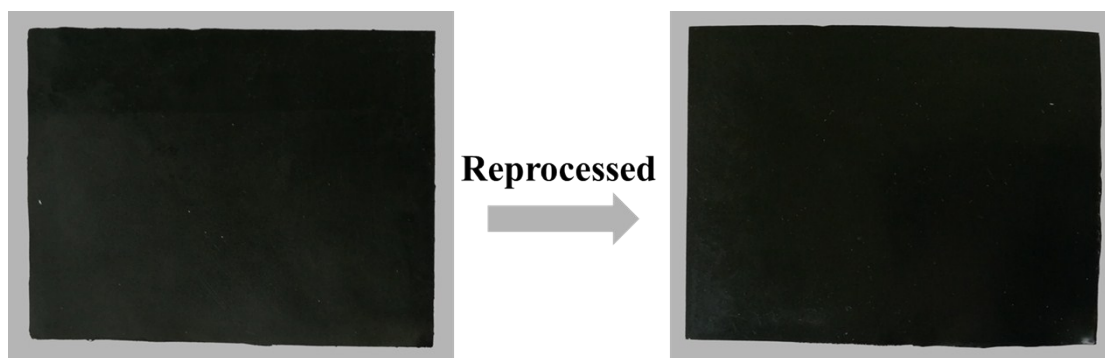


Fig. S9. Photograph of the original (left) and the reprocessed (right) rubber films by hot pressing at 180 °C.

18. Mechanical properties of original and recycled CB-x composites

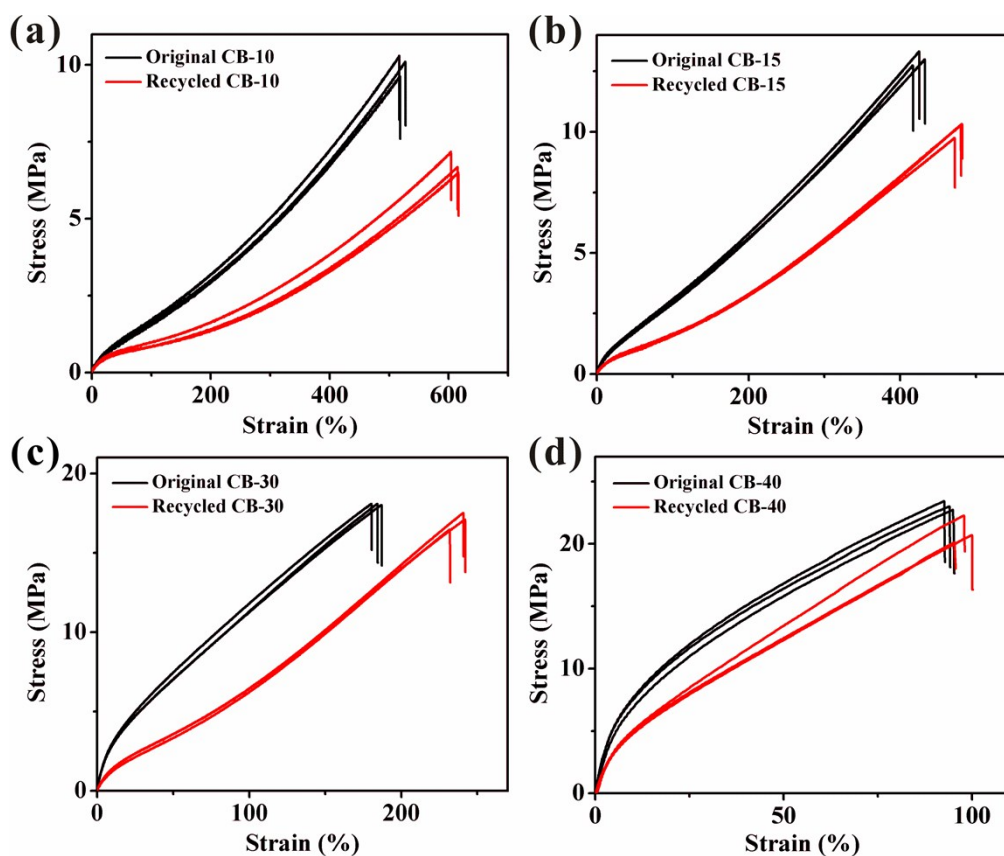


Fig. S10. Stress-strain curves of original and recycled CB-10 a), CB-15 b), CB-30 c) and CB-40 d).

Table S7. Recovery of mechanical properties of CB-x samples after reprocessing

Samples	Recovery of	Recovery of	Recovery of 100%
	Tensile Strength (%)	Elongation at Break (%)	Tensile Modulus (%)
CB-10	$(70 \pm 4)\%$	$(117 \pm 3)\%$	$(56 \pm 5)\%$
CB-15	$(77 \pm 3)\%$	$(113 \pm 2)\%$	$(54 \pm 1)\%$
CB-20	$(83 \pm 1)\%$	$(118 \pm 6)\%$	$(53 \pm 4)\%$
CB-30	$(91 \pm 3)\%$	$(126 \pm 5)\%$	$(55 \pm 2)\%$
CB-40	$(89 \pm 9)\%$	$(101 \pm 5)\%$	/

19. FTIR spectra and cross-linking density of original and recycled CB-20

Compared with the original sample, the absorption intensity of carbonyl in ester bond centered at 1730 cm^{-1} exhibits an apparent decline after the reprocess of CB-20 sample., indicating the insufficient transesterification reactions during reprocessing. This should be ascribed to high activation energy in the present system and the short reprocessing time (15 min) during reprocessing.

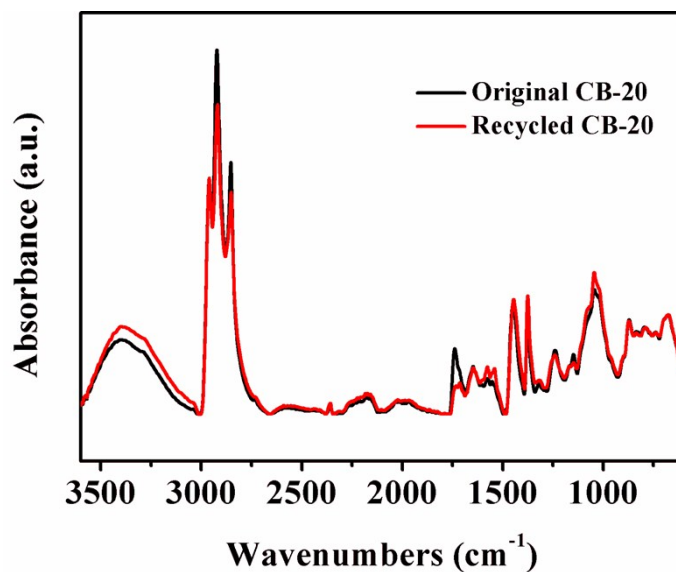


Fig. S11. FTIR spectra of original and recycled CB-20.

Table S8. Cross-linking densities of original and recycled CB-20 samples

	Cross-linking density (10^{-5} mol/cm^3)
Original CB-20	19.4
Recycled CB-20	11.2

20. References

1. M. E. Lipińska, S. L. H. Rebelo, M. F. R. Pereira, J. A. N. F. Gomes, C. Freire and J. L. Figueiredo, *Carbon*, 2012, **50**, 3280-3294.
2. M. Pire, S. Norvez, I. Iliopoulos, B. L. Rossignol and L. Leibler, *Polymer*, 2011, **52**, 5243-5249.
3. M. Pire, S. Norvez, I. Iliopoulos, B. L. Rossignol and L. Leibler, *Compos. Interface.*, 2014, **21**, 45-50.
4. M. Capelot, D. Montarnal, F. Tournilhac and L. Leibler, *J. Am. Chem. Soc.*, 2012, **134**, 7664-7667.
5. M. Capelot, M. M. Unterlass, F. Tournilhac and L. Leibler, *Acs Macro Letters*, 2013, **1**, 789-792.
6. Y. X. Lu, F. Tournilhac, L. Leibler and Z. Guan, *J. Am. Chem. Soc.*, 2012, **134**, 14226-14231.
7. P. J. Flory and J. Rehner, Jr, *J. Chem. Phys.*, 1943, **11**, 512-520.
8. P. J. Flory, *J. Chem. Phys.*, 1950, **18**, 108-111.
9. H. Nabil, H. Ismail and A. R. Azura, *J. Elastom. Plast.*, 2011, **43**, 429-449.
10. Y. Liu, Z. Tang, Y. Chen, C. Zhang and B. Guo, *ACS. Appl. Mater. Inter.*, 2017, **10**, 2992-3001.
11. T. Stukenbroeker, W. Wang, J. M. Winne, F. E. D. Prez, R. Nicolaÿ and L. Leibler, *Polym. Chem-UK.*, 2017, **8**, 6960-6953.
12. H. Zhang, D. Wang, N. Zhao and J. Xu, *J. Polym. Sci. Pol. Chem.*, 2017, **55**, 2011-2018.
13. P. Yan, W. Zhao, Y. Wang, Y. Jiang, C. Zhou and J. Lei, *Macromol. Chem. Phys.*, 2017, **218**, 1700265.
14. Z. Q. Lei, H. P. Xiang, Y. J. Yuan, M. Z. Rong and M. Q. Zhang, *Chem. Mater.*, 2014, **26**, 2038-2046.
15. L. Imbernon, E. Oikonomou, S. Norvez and L. Leibler, *Polym. Chem-UK.*, 2015, **6**, 4271-4278.
16. H. P. Xiang, H. J. Qian, Z. Y. Lu, M. Z. Rong and M. Q. Zhang, *Green. Chem.*, 2015, **17**, 4315-4325.
17. Q. Shi, K. Yu, M. L. Dunn, T. Wang and H. J. Qi, *Macromolecules*, 2016, **49**, 5527-5537.